Isothermal ramped field-desorption of water from metal surfaces

A. Stintz and J. A. Panitz
Department of Physics and Astronomy, University of New Mexico, Albuquerque, New Mexico 87131

(Received 10 February 1992; accepted for publication 30 March 1992)

It is shown that water vapor deposited onto metal surfaces between 80 and 130 K can be isothermally desorbed by applying a ramped electric field. At a ramp rate of ~1 MV/cm/s the desorption field strength for physisorbed layers of amorphous ice on tungsten and iridium surfaces is ~80 MV/cm. As the ice layers desorb in the presence of the high electric field, positive ions are formed which are detected. During this process, the ice exhibits properties of an electrical conductor or a semiconductor.

I. INTRODUCTION

The liquid-solid interface is of fundamental interest in the scientific community. Numerous authors have investigated the interaction of water with solids. A recent comprehensive review on the subject is given in an article by Thiel and Madey.[1] For example, water on surfaces plays a key role in corrosion and catalytic processes. One of the techniques to study the binding properties of water adsorbed on metal surfaces is thermal desorption spectroscopy (TDS), where the adsorbate is desorbed by increasing the temperature of the substrate in a controlled way.[2] In this publication, a ramped electric field is applied to a water-solid interface, producing spectra similar to those obtained by TDS, but under isothermal desorption conditions.[3,4] Water is preadsorbed on a solid surface at cryogenic temperatures and desorbed isothermally by applying a high electric field whose magnitude increases linearly with time. Positive ions are produced from the field-desorbed layer and detected as a function of the applied field strength.

II. EXPERIMENTAL DETAILS

Since the electric field, F, required to desorb species from surfaces is of the order of 100 MV/cm, a field emitter needle with a radius of curvature, R, of around 100 nm is used as a substrate. Applying a high voltage ($V \sim 5$ kV) to the needle creates the required field at its apex according to the relation:[5]

$$F \sim V/5R. \tag{1}$$

The experimental arrangement is shown schematically in Fig. 1. A field emitter tip is mounted in a UHV chamber and can be turned during an experiment so that it faces an ion detector or the capillary tube of a water dosing assembly. The tip is held at a temperature of ~80 K by a cold finger filled with liquid nitrogen, but it can also be heated by passing an electric current through a wire loop which supports the tip. A thermocouple wire spotwelded onto the tip monitors the tip temperature. Water is introduced on the tip surface by closing valve (A) which connects the dosing assembly with the pump, opening valve (B) to the H_2O reservoir, and turning the tip towards the capillary tube. The tip is exposed to the water vapor emerging from the capillary tube for a definite amount of time at a certain water pressure in the dosing assembly chamber. To stop the water deposition on the tip the above procedure is reversed. Now a high voltage, linearly increasing with time, is applied to the tip. This causes the electric field on the tip apex to rise linearly with time according to Eq. (1). When the field reaches the value required to ionize the water molecules, positive ions are created and accelerated radially away from the tip towards a channel electron multiplier assembly (CEMA). The CEMA output signal is proportional to the number of arriving ion species and is recorded as a function of the electric field to produce a spectrum. The CEMA also produces a magnified image of the tip surface on a phosphor screen with sub-nanometer resolution.[6] As a result, the spatial distribution of the arriving ion species can also be studied as a function of the applied field.

The water used in this experiment was freshly distilled, and then frozen and thawed in vacuum several times to eliminate dissolved residual gases. The water reservoir was kept at room temperature during these experiments. The experiments were performed at a base pressure of 2×10^{-8} Torr or better. The pressure rose during the dosing of the water up to 10^{-7} Torr, but typically recovered within a minute, after which the field was applied.

Prior to the dosing, the tips were imaged and field-evaporated in 10^{-4} Torr helium to clean and smooth the surface and to obtain a voltage-field calibration. Field evaporation occurs at ~570 MV/cm for tungsten in vacuum at 77 K.[7] With the known corresponding voltage, the proportionality constant $5R$ is determined from Eq. (1), allowing the electric field on the tip apex to be calculated for arbitrary voltages. It should be noted that the evaporation fields for most metals are only known to an accuracy of ~15%. The presence of helium lowers these fields by an additional amount.[7] Therefore, the electric field strength data presented here are only accurate to ~20%. The ratios of two fields on the same specimen tip, however, are reproducible to better than 5%.

III. RESULTS

Figure 2(a) shows a spectrum of field-desorbed H_2O from tungsten at 80 K after 30 s exposure to water vapor with the water pressure in the dosing assembly chamber being 0.05 Torr. The number of ions counted is plotted

 0021-8979/92/140741-05$04.00

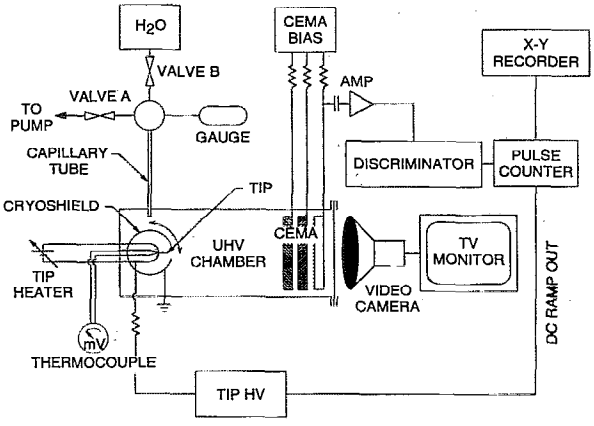

FIG. 1. Experimental arrangement. A cooled field emitter tip in UHV is coated with vitreous ice and then turned towards an ion detector. A voltage ramp is applied to the tip and the ion output is recorded.

versus the electric field strength. The broad peak is attributed to the removal of physisorbed multilayers of water from the substrate surface by field desorption. Video images show that the spatial distribution of the ions is uniform until the peak reaches its maximum. Then, the water layer seems to "peel" away from near the center or (110)-plane of the tip, occasionally leaving random emission sites behind. The desorption field strength lies between 80 and 100 MV/cm; a more careful investigation with low doses of water shows that the onset of the desorption is close to 70 MV/cm [Fig. 2(b)]. Spectra were also taken from water adsorbed on an iridium substrate [Fig. 2(c)]. The desorption field is estimated to be in the same range as for tungsten. A distinguishing feature is that the first peak shows two maxima in close proximity, and when the field is increased above ~ 100 MV/cm random ion emission occurs. All spectra in Fig. 2 were taken at a ramp rate of the electric field of ~ 1 MV/cm/s.

A series of experiments was performed to investigate the influence of the amount of water coverage on tungsten. Spectra were obtained for different exposure times, namely 4, 8, 15, 30, 60, and 120 s. The areas under the peaks, which correspond to the total ion yield, were determined. They are close to the expected linear dependence on exposure time up to 1 min (Fig. 3). At 2 min and above, the spectra were not reproducible, probably due to thick coverages of water.

An attempt was made to estimate the layer thickness. The onset voltage of the desorption was determined as a function of exposure time (Table I). Onset voltage versus exposure time exhibit a linear relationship. The motivation for this study was the following. Assuming that the water layer is uniform, the electric field, F, acting on the outside of a dielectric layer around a field emitter tip is given by

$$F=[\epsilon R/(\epsilon R+d)]V/k(R+d), \qquad (2)$$

where ϵ is the relative dielectric constant of the layer, R the radius of the tip, d the layer thickness, V the applied voltage, and k a geometrical factor.[8] Here, with $\epsilon \sim 100$, $R > d$,

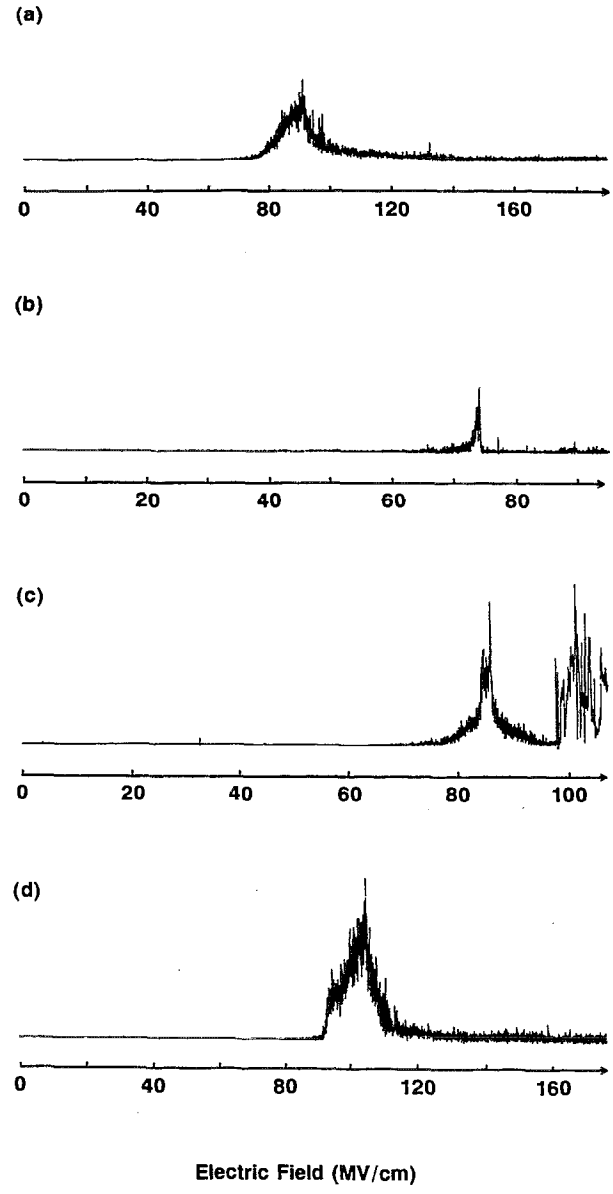

FIG. 2. Ion yield from the field-desorbing water layer as a function of field strength for (a) H_2O on W, (b) low coverage of H_2O on W, (c) H_2O on Ir, all at 80 K, and (d) H_2O on W at 125 K.

and $k \sim 5$, we get $F \sim V/5(R+d)$.[9] Unfortunately, the data in Table I are within a 5% error resulting from possible changes in the tip radius itself. Therefore, an alternate approach was used.

A commercial quartz crystal deposition monitor was used to measure the layer thickness.[10,11] The crystal was mounted in the UHV chamber in place of the field emitter tip (Fig. 1) and cooled to 80 K. H_2O is sprayed onto the surface of the cooled crystal. The dosing conditions are similar to the ones in the desorption experiment: The dosing time is 30 s, the pressure of the H_2O in the dosing chamber is 0.05 Torr, and the distance from the orifice of the capillary tube to the crystal is about four times the distance from the orifice of the capillary tube to the field emitter tip. This ensures that the crystal is covered with

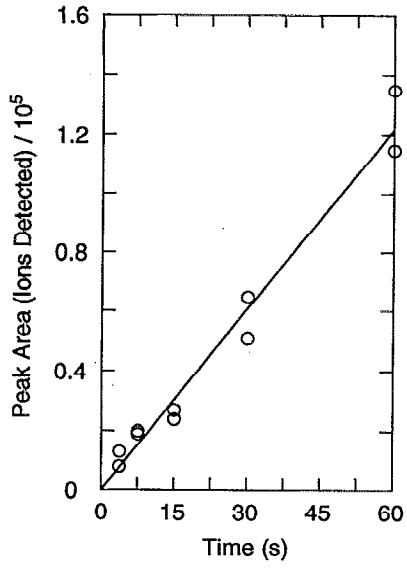

FIG. 3. Ion yield from the field desorption of H_2O as a function of exposure time.

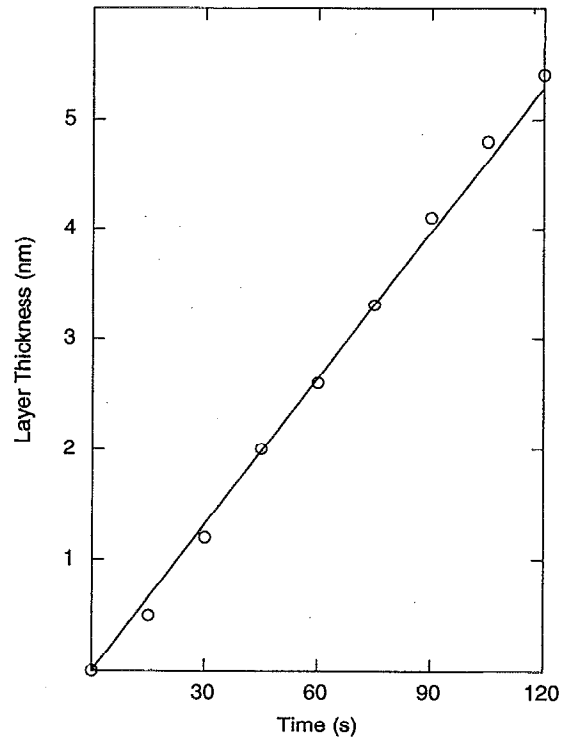

FIG. 4. H_2O layer thickness vs exposure time; layer thickness measured with an oscillating quartz crystal.

H_2O more uniformly and not only in the middle. The difference in oscillation frequency of the crystal before and after depositing the H_2O layer is converted into an average thickness reading of the ice layer, using a density of amorphous ice of 0.93 g/cm^3.[12] The average ice thickness on the crystal obtained this way is 1.2 ± 0.2 nm. This implies that the H_2O coverage on the specimen tips at these dosing conditions was ~ 20 nm, assuming a quadratic dependence of the coverage on distance. In the same way, H_2O thickness measurements were made with dosing times in the range from 15 s to 2 min (Fig. 4). The graph shows a linear increase in thickness of the ice layer on the quartz crystal with time.

The adsorption of water was also studied as a function of the temperature of the tungsten substrate. The water was sprayed onto the tungsten tip for 30 s while the tip was held at a constant temperature between 80 and 170 K. One minute after the deposition, the temperature was lowered to 80 K to minimize surface migration of the water on the tip while raising the electric field. Then the spectra were taken. No drastic changes were observed up to a temperature of ~ 130 K. However, near 130 K the peak exhibits a more distinct initial rise, and its onset is slightly shifted towards higher voltages [Fig. 2(d)]. In the range between ~ 135 to ~ 160 K the spectra changed and were not reproducible within the accuracy of our temperature measurement (± 5 K). Sometimes sharp peaks would appear well below the calculated desorption field strength of 80 MV/cm, similar to our observations with thick water layers. At other times, the area under the major peak was considerably less than for the spectra recorded below 130 K. Above ~ 160 K, no adsorbed water could be detected above the background noise level.

TABLE I. Onset voltage, V, of desorption vs exposure time, t, of the substrate to H_2O vapor.

t/s	4	8	15	30	60
(1) V/kV	2.35	2.35	2.37	2.41	2.50
(2) V/kV	2.33	2.35	2.36	2.43	2.48

IV. DISCUSSION

Water sprayed onto a surface below 130 K (i.e., at liquid nitrogen temperature) forms an amorphous or vitreous ice layer.[9,12] Hexagonal water ice at this temperature is thought to be an electric insulator from extrapolation of known data to lower temperatures.[13] Insulating layers on field emitter tips are not removed smoothly as a function of applied field.[8] Yet, the desorption process observed here is smooth. This suggests that the ice layer is at least semiconducting when it is removed by the electric field. Then why does this experiment work? Two possibilities arise.

(1) Amorphous ice may have different electrical properties than hexagonal ice. Perhaps the activation energy for charge carriers is very small, so that electrical conduction can occur even at low temperatures. It is well known that the energy bands in amorphous semiconductors are different from those in a crystalline state.[14] To our knowledge, no dc-conductivity measurements have been made for thin vitreous layers of water ice as produced in this experiment.

(2) The charge carriers in the ice layer are produced by a field-dissociation effect, which was first described by Onsager[15] and also considered as an explanation in extensive studies of field-ionization of water.[16] The mechanism may be represented by the reaction

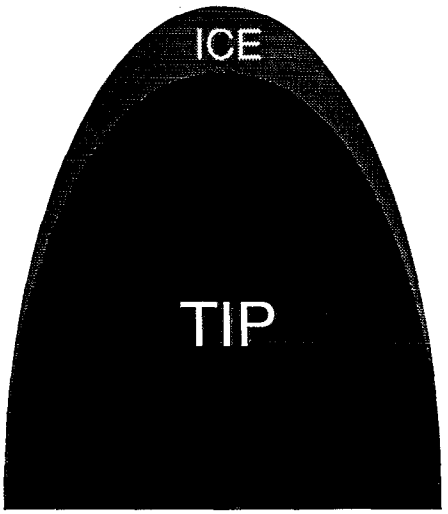

FIG. 5. Probable configuration of an amorphous ice layer on a field emitter tip at 80 K after vapor deposition in UHV.

$$2H_2O \rightarrow H_3O^+ + OH^- \quad (3)$$

with only the positive ions created being detected by our apparatus. Mass spectrometry of the field-desorbed ions is in progress to investigate this possibility. It is possible that cluster ions are also produced, as observed in similar studies, especially at low temperatures.[17]

The threshold field for the field desorption of the ice layer is with 80 MV/cm, more than three times as high as it is for the ionization of water on a tungsten field emitter at room temperature with a continuous water supply.[18] Moreover, no significant change was observed with an iridium substrate. It is therefore believed that the majority of the field-desorbed water was truly physisorbed and did not interact with the metal surface. Possibly the first few atomic layers of ice may have reacted with the tungsten surface and formed oxides and/or hydrides. This reaction is known to take place at room temperature,[19] and it occurs at other metal surfaces even below 100 K.[20] However, the effect here was not such that a change in tip radius could be detected within 5%.

As mentioned earlier, due to our inability to detect tip radius changes this small, the ice layer thickness cannot be determined from Table I. Moreover, it is not possible to set a reasonable upper limit for the following reason: In the deposition process, the water molecules hit the tip preferentially from the front. Instead of forming a uniform layer around the tip, the deposit will preferentially build up on the apex of the tip, leaving the shank almost ice free (Fig. 5). Therefore, even with thick ice deposits, the radius of curvature at the ice-vacuum interface would not change appreciably. With the large dielectric constant of ice, the field acting on the ice surface at a fixed voltage would thus be about the same for thin and thicker layers. That the representation of the ice layer in Fig. 5 is probably correct is consistent with the data on the layer thickness measurement with the oscillating quartz crystal. The film thickness monitor data give an approximate thickness of the H_2O layer desorbed in Fig. 2(a) of $\sim$20 nm. This value should be treated with some caution, because:

(1) The film thickness monitor is designed to work at room temperature. Theoretically, the principle of the measurement is the same for different temperatures. We experienced a frequency shift during the cooling process of the crystal. It indicated that the frequency change due to the cooling was less than 0.1% which is well within the operating range of the instrument. After the frequency stabilized at liquid nitrogen temperature, a measurement became possible.

(2) The film thickness reading is an average over the entire central region of the quartz crystal (area $\sim$20 mm^2). The field emitter tip (apex area $\sim 10^{-8}$ mm^2) could have a different layer thickness than the average reading due to variations in the angular distribution of the water vapor emerging from the capillary tube. An estimated error as large as 50% may arise from this effect.

The desorption spectra are not reproducible for thick coverages of water and for temperatures above $\sim$130 K. It is known that raising the temperature of amorphous ice above $\sim$130–135 K causes the ice to transform into a cubic crystalline form.[21] Also, above this temperature, condensing water will form cubic rather than amorphous ice and stay cubic after cooling it below 130 K. Perhaps the crystallization introduces a surface roughness or even growth of needles, similar to what is observed with vapor deposited salt on field emitter tips.[22] This could introduce local field enhancements, explaining sporadic ion detection at lower than threshold voltages. When a thick layer is building up, the arriving water molecules are at room temperature when they hit the already existing ice layer. Since the thermal conductivity of ice is much poorer than that of a metal, the temperature could locally rise above 130 K, inducing crystal growth. It seems plausible that slightly below this transition temperature surface migration of the H_2O molecules plays a role and makes the ice surface more uniform, explaining our findings in Fig. 2(d).

The complete absence of water in the spectra above $\sim$160 K is consistent with previous data on thermal desorption spectroscopy of water,[20] where the physisorbed water desorbs from the surface in a temperature range around 160 K.

Future experiments are planned to determine the composition of the emerging ion species using mass spectroscopy, similar to mass resolved thermal desorption spectroscopy. The field-desorption of the ice layer will also be studied by applying a high voltage pulse with a rise time of $\sim$1 ns to the specimen.

ACKNOWLEDGMENTS

We wish to thank Jim Hontas, Jesus Sanchez, and John DeMoss from the Physics and Astronomy machine shop for machining part of our instrumentation. This work was supported by the United States Department of Energy (Office of Basic Energy Sciences) under DOE Grant DE-FG04-88ER45348.

[1] P. A. Thiel and T. E. Madey, Surf. Sci. Rep. **7**, 211 (1987).
[2] See, for example, P. A. Redhead, Vacuum **12**, 203 (1962); G. Ehrlich, Adv. Catal. **14**, 255 (1963).
[3] J. A. Panitz, J. Vac. Sci. Technol. **16**, 868 (1979).
[4] K. D. Rendulic and M. Leisch, Surf. Sci. **93**, 1 (1980).
[5] R. Gomer, *Field Emission and Field Ionization* (Harvard University Press, Cambridge, MA, 1961).
[6] E. W. Müller and T. T. Tsong, Prog. Surf. Sci. **4**, 1 (1973).
[7] E. W. Müller and T. T. Tsong, *Field Ion Microscopy, Principles and Applications* (Elsevier, New York, 1969).
[8] A. L. Pregenzer, K. W. Bieg, R. E. Olson, and J. A. Panitz, J. Appl. Phys. **67**, 7556 (1990).
[9] N. H. Fletcher, *The Chemical Physics of Ice* (Cambridge University Press, Cambridge, MA, 1970).
[10] G. Sauerbrey, Z. Physik **155**, 206 (1959).
[11] Thin film thickness monitor, manufactured by Inficon Leybold-Heraeus Inc., Model No. 751-001-G1.
[12] J. Dubochet, J.-J. Chang, R. Freeman, J. Lepault, and A. W. McDowall, Ultramicroscopy **10**, 55 (1982).
[13] M. Durand, M. Deleplanque, and A. Kahane, Solid State Commun. **5**, 759 (1967).
[14] See, for example, H. Overhof and P. Thomas, *Electronic Transport in Hydrogenated Amorphous Semiconductors* (Springer, Berlin, 1989).
[15] L. Onsager, J. Chem. Phys. **2**, 599 (1934).
[16] See, for example, F. W. Röllgen and H. D. Beckey, Surf. Sci. **27**, 321 (1971), and references therein.
[17] H. D. Beckey, Z. Naturforsch. **15a**, 822 (1960).
[18] W. A. Schmidt, Z. Naturforsch. **19a**, 318 (1964).
[19] See, for example, H. Imai and C. Kemball, Proc. R. Soc. (London) A **302**, 399 (1968).
[20] Ref. 1 and references therein.
[21] J. Dubochet, J. Lepault, R. Freeman, J. A. Berriman, and J.-C. Homo, J. Microsc. **128**, 219 (1982).
[22] P. R. Schwoebel and J. A. Panitz, J. Appl. Phys. **71**, 1 (1992).